

Brushless Synchronous Generator Turn-to-Turn Short Circuit Fault Detection Using Multilayer Neural Network

Pyae Phyo Tun
Rolls-Royce @ NTU Coporate Lab
Nanyang Technological University,
Singapore

Liu Shuyong
Rolls-Royce Singapore Pte Ltd,
Singapore

Padmanabhan Sampath Kumar
Rolls-Royce @ NTU Coporate Lab
Nanyang Technological University,
Singapore

Ryan Arya Pratama
Rolls-Royce @ NTU Coporate Lab
Nanyang Technological University,
Singapore

Abstract— Stator winding short circuit is one of the faults that occur frequently in electrical machines. Therefore, fault detection and elimination in electric drive systems is necessary for safety-critical applications in order not to cause catastrophic failure to the machine in a short time. This paper reviews recent fault detection and diagnosis techniques that use signal analysis, model-based techniques and artificial intelligence machine diagnosis methods. Then, feedforward neural network will be trained, tested and validated whether or not this artificial neural network can classified healthy and different severity inter-turn short circuit levels by using per unit RMS 3 phases current and voltage quantities as well as fundamental and third harmonic components of current and voltage.

Keywords—component; brushless synchronous generator, power generation, condition monitoring, fault detection, fault diagnosis, artificial neural network, electrical machine.

I. INTRODUCTION

The brushless synchronous generators are widely used to power aircrafts, ships and trains. Therefore, it is necessary to improve reliability of the operation of these generators in order to run continuously and safely in mission critical applications. Different types of electrical and mechanical faults such as turn-to-turn winding short circuit fault, bearing fault, broken rotor bar fault [1]-[4], and so on can be occurred in electrical machines due to harsh environmental conditions and system stress like extreme ambient temperature range, high humidity, dust, overloading, severe duty cycle [5], and so on. All of these faults are inherent to the machine as incipient fault. Failure to detect and eliminate faults at its early stage allows faults to grow and eventually it will create catastrophic failure of machine.

Electrical fault especially stator winding related faults are one of the most common faults and one of the most difficult failures to detect in electrical machine [4],[6],[7]. Stator winding faults generally comprises turn-to-turn short circuit fault, phase-to-phase fault, and phase-to-ground fault. High stator core or winding temperature, day-to-day accumulation of oil, moisture and dirt particles, and partial discharges cause insulation failure between two adjacent stator windings [6]. This will create high circulating current, local heating and imbalance in magnetic field in the machine. If this turn-to-turn short circuit fault is not detected early, the fault will grows into phase-to-phase fault, and then phase-to ground fault, and finally, it will severely damage to the machine and cause unexpected shutdown. Thus, better fault-detection and

rectification strategies are required in safety-critical applications.

Condition Based Monitoring (CBM) scheme predicts the operational and possible failure of machine at its early stage based on measured machine's electrical and physical phenomena such as current, voltage, sound, vibration, temperature, and so on. Therefore, condition based maintenance outweighs traditional schedule maintenance scheme in many ways. Condition based maintenance scheme can detect both machine's electrical and mechanical faults as early as possible. Hence, machine downtime can be reduced and this will improves productivity, safety, energy efficiency and saves maintenance cost [8]. In addition, with condition based maintenance scheme, machine can be operated for its whole service lifetime at minimum operation cost [8]. Customer also will have an opportunity to adjust maintenance intervals based on condition of machine.

Several different machine condition monitoring techniques have been used in literature. In reference [9], the stator winding fault in the brushless synchronous generator (BLSG) is detected by using harmonic spectral analysis (e.g. Fast Fourier Transform or short-time Fourier Transform) of vibration signal. In addition, in reference [6], the inter-turn stator winding fault in motor is detected and localized by recognizing deformation Concordia pattern of instantaneous spatial vector sum of the 3 phase stator currents. Reference [8] also suggests that machine terminal voltage harmonic analysis and instantaneous active and reactive power analysis can be used in inter-turn fault detection. Signal based analysis using current and voltage signals is cheap, but it is not suitable to use in variable speed and load applications [13].

Furthermore, process model-based fault detection technique makes use of mathematical modelling to aid the study of stator turn-to-turn short circuit fault in electrical machine [13], [14]. Parameter estimation [14], and state observation methods [14] are widely used to observe fault symptoms. The benefits of using a machine model-based fault detection technique are: it allows early detection of incipient stator fault under speed and load variations [14], [4], it also provides flexibility of simulating different machines by changing parameters of model [13], it is cheap and convenient method for testing a fault-diagnosis algorithms [13] and it can be applied in either offline or online stator fault-detection [13]. However, the drawbacks of this technique are: it is sensitive to noise [15], when nonlinearities exist, analytical approaches may not model a

machine accurately, and inaccurate model could create error during fault identification process [13], [4].

The artificial intelligence techniques such as neural network, fuzzy logic, support vector machine, and so on can be used as a machine diagnostics tool. Artificial intelligence machine diagnosis methods treat the system as input-output map and hence dynamic machine model is not required and uncertainty in model output due to nonlinearities can be eliminated. In [6] and [7], induction motor speed, current and voltage parameters are used to train feedforward neural network with Levenberg Marquardt gradient decent algorithm in order to detect fault in induction motor. In [11], stator current in time domain from faulty and healthy induction motor is input to the artificial neural network, which will identify the short circuit fault by learning stator current patterns.

This paper investigates turn-to-turn short circuit fault detection in Brushless Synchronous Generator by using multi-layer neural network back propagation algorithm because the proposed technique does not required detailed analysis of different kinds of faults or modelling of the system. This paper also studies the effects of different types of input features and different numbers of hidden layer neurons on neural network performance. In this paper, six different severity levels of inter-turn stator winding faults plus healthy stage of the brushless synchronous generator are classified by using pattern recognition network also known as feedforward network [12]. In this supervise learning, first machine healthy state and six different severity levels of turn-to-turn stator winding faults are introduced in every 10s interval. Then, the pattern recognition network is trained to classify inputs – per unit RMS values of current and voltage as well as fundamental and third harmonic components of current and voltage – according to target classes – healthy machine and inter-turn short circuit fault level 1 to 6.

This article is organized as follow: section 2 will present the experimental setup for current and voltage data acquisition. Then, section 3 will describe overall system architecture of the neural network followed by feature extraction for neural network algorithm. Section 5 will explain about feed forward neural network. Section 6 will present experimental results on inter-turn short circuit stator winding faults by using neural network. Finally, in section 7, the conclusion of the study will be presented.

II. EXPERIMENT SETUP

Experiment setup consists of 14 kVA 3 phase synchronous generator connected to linear load, turn-to-turn stator winding fault emulation test rig, and National Instrument data acquisition system. 3 phase current and voltage data are acquired at 10 kHz with National Instrument data acquisition system for 69s. Fig. 1 shows the experiment setup.

Next, 10% of synchronous generator V phase winding, as shown in fig. 2, is tapped out to introduce different severity level of short circuit by decreasing short circuit resistance, R_f value. Table 1 shows test profile for stator winding fault.

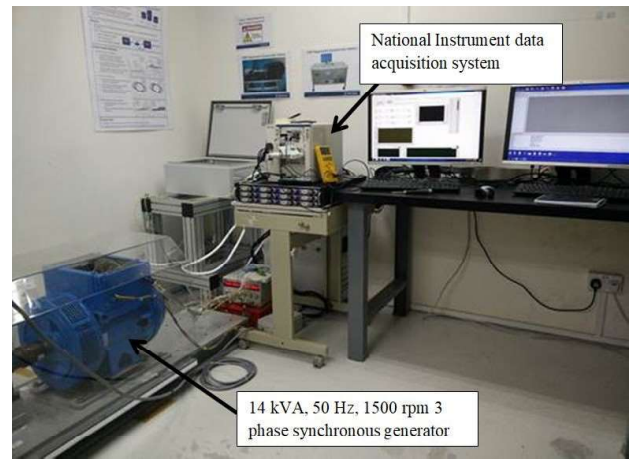


Fig. 1. Experiment setup

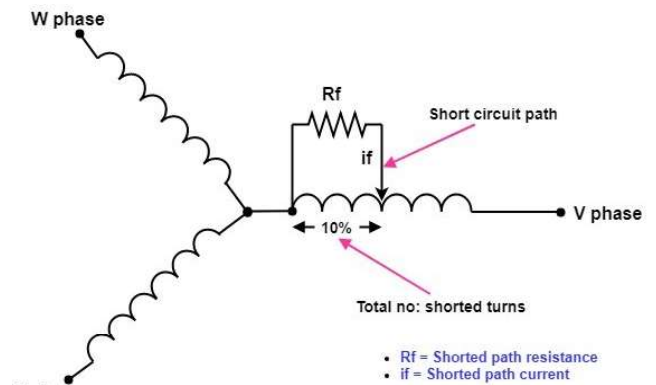


Fig. 2. Stator winding with short circuit in V phase

Table 1. Test Profile of turn-turn short circuit fault

Test duration	Effective short circuit resistance, R_f , in Ω
00 s – 09 s	∞ (Healthy)
09 s – 19 s	50 (Stator winding short circuit fault level 1)
19 s – 29 s	25 (Stator winding short circuit fault level 2)
29 s – 39 s	12.5 (Stator winding short circuit fault level 3)
39 s – 49 s	6 (Stator winding short circuit fault level 4)
49 s – 59 s	3 (Stator winding short circuit fault level 5)
59 s – 69 s	1.5 (Stator winding short circuit fault level 6)

III. SYSTEM DESCRIPTION

In general, machine learning algorithm consists of learner and reasoner. Learner builds model by learning given data and background knowledge. This model is then used by reasoner to provide prediction or classification. Fig. 3 shows the schematic block diagram of supervise learning.

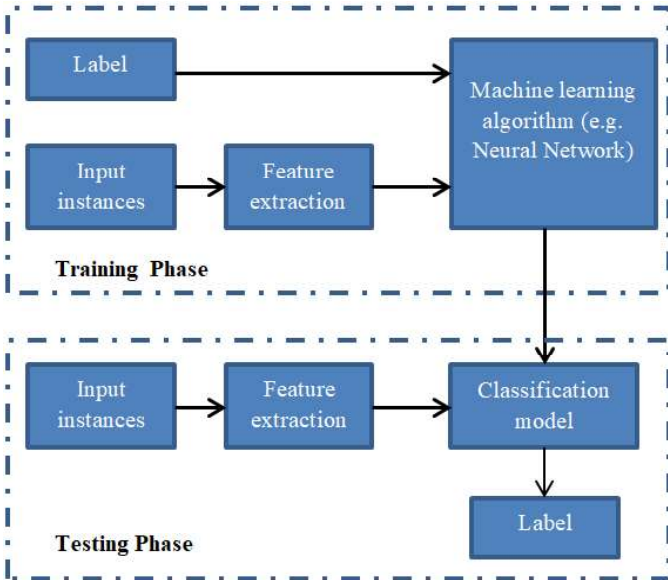


Fig. 3. Schematic diagram of supervised learning

The workflow consists of data exploration, data labelling, model development, training and testing model. In the data exploration phase, data from sensors are transformed into valid and clean data format which are ready to use as input to the model training. This step involves data acquisition, feature extraction, normalization and labelling data. First of all, electrical signal such as 3 phases current and voltage are collected from machine at 10 kHz by using National Instrument data acquisition system. Then, different data attributes like RMS values of current and voltage signal, and different frequency components of current and voltage are extracted from raw data which will be used in developing model. After that, all these numeric data are normalized to a common scale followed by labelling those data instances. After necessary data pre-processing has been done, two layer feedforward pattern recognition neural network model [12] is developed. Then, this learning algorithm is trained by feeding the data with known target value. As a result, it will generate classification model which is good enough for the needs of application. Trained model is then evaluated by using different data set like training data set and compared model's prediction and actual values for the evaluation data. Finally, test the classification model with different set of test data which has never processed before. This classification model will predict label corresponding to respective input data instances.

IV. FEATURE EXTRACTION

The acquired time domain signal of current and voltage signal from synchronous generator are decomposed into different distinctive features such as per unit RMS values, fundamental and third harmonic components of current and voltage signal. These representative features can be used by machine learning algorithm to generate classification model which can be classify input data into different classes with minimum error. Fig. 4 shows per unit RMS value of current and voltage. Moreover, in order to process all extracted features in same scale, the harmonic component values of current and voltage are normalized. Fig. 5, and 6 show normalized value of fundamental and third harmonic components of current and voltage.

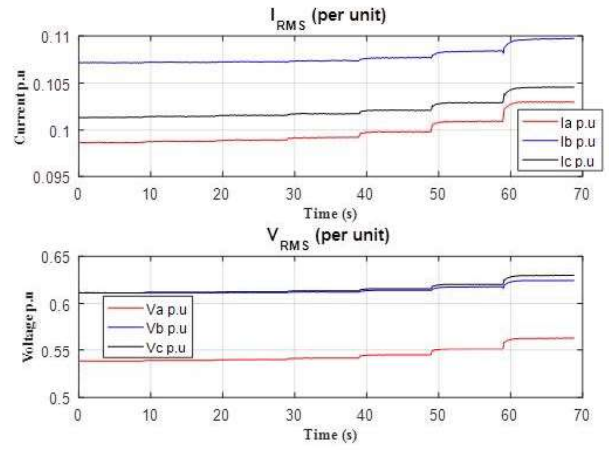


Fig. 4. Per unit value of current and voltage

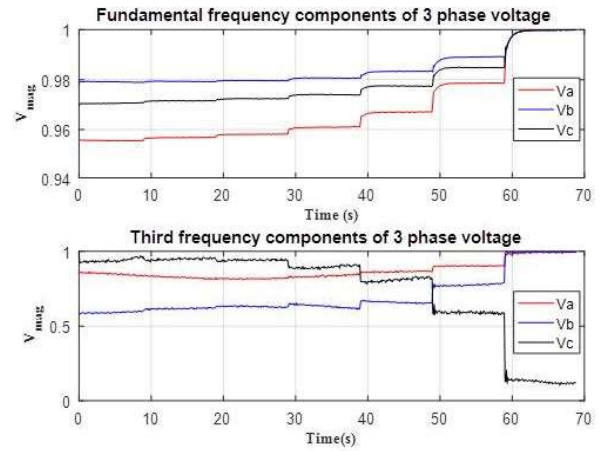


Fig. 5. Fundamental and third harmonic components of 3 phase voltage after normalization

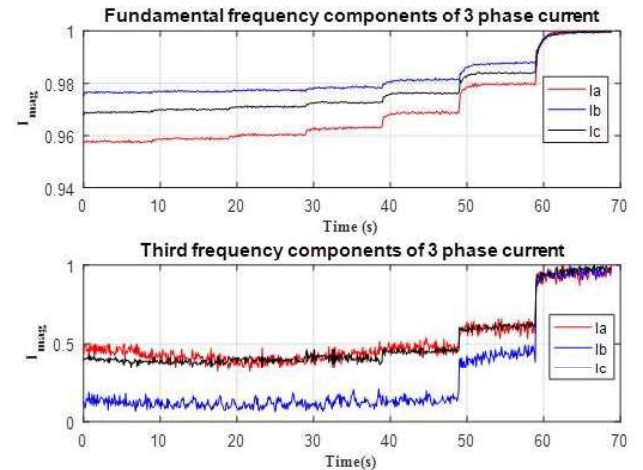


Fig. 6. Fundamental and third harmonic component of 3 phase current after normalization

V. ARTIFICIAL NEURAL NETWORK

Generally, a perceptron unit of artificial neural network is first computed the weighted sum of each and every input values ($x_1, x_2, x_3 \dots x_n$) and then they are passed into activation unit. The transfer function of an activation unit can be linear function, or thresholding function or sigmoid

function. Fig. 7 illustrates a representation of the artificial neuron.

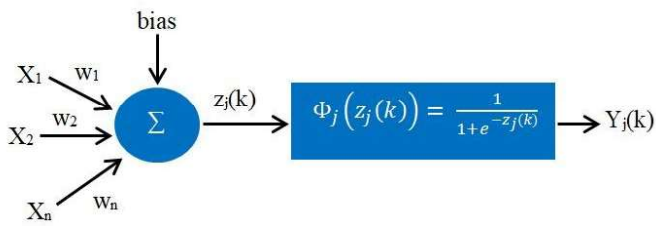


Fig. 7. Representation of artificial neuron

Moreover, feedforward neural network can have multi-layer. In multi-layer neural network, any number of hidden layers can be included between input and output. Fig. 9 shows 2 layer fully connected feed-forward backpropagation neural network. Two layers feedforward neural network consists of 1 hidden layer and 1 output layer between input and output. In fig. 9, it can be seen that in multilayer neural network, computation in network moves from input to output, whereas errors which are observed at the output is propagated backward. Like single layer perceptron, the value of weight in each stage will be updated every iteration based on error in output.

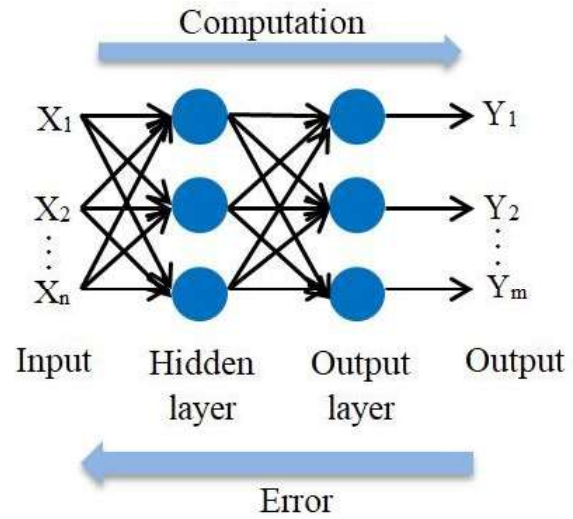


Fig. 9. Two layers back propagation neural network

Fig. 8 shows flowchart of feedforward neural network. The feedforward neural network algorithm starts with initializing initial values of weight between input and hidden layers. After that, output values in successive layers are calculated for training inputs; and then, error in the output is calculated based on model's predictions and target values. This error signal is back propagated from output to hidden layers and then to input. Based on that error value, weights and bias values between hidden layer and input are adjusted to minimize error values. Once optimal performance is achieved, which means error value is minimum, training will be stopped and generated model is ready to use for testing and deployment.

In this project, two layers neural network is used to train different combination of features data set in MATLAB programming environment to classify different stages of synchronous generator - healthy condition, and inter-turn short circuit with different severity level conditions. Experimental results and analysis will be presented in next section.

VI. CLASSIFICATION OF TURN-TO-TURN SHORT CIRCUIT FAULT USING MULTILAYER NEURAL NETWORK

This section will illustrate about experimental results of classification of different conditions of synchronous generator – **class 1** (Healthy); **class 2** (short circuit fault level 1, $R_f = 50 \Omega$); **class 3** (short circuit fault level 2, $R_f = 25\Omega$); **class 4** (short circuit fault level 3, $R_f = 12.5 \Omega$); **class 5** (short circuit fault level 4, $R_f = 6\Omega$); **class 6** (short circuit fault level 5, $R_f = 3\Omega$) and **class 7** (short circuit fault level 6, $R_f = 1.5\Omega$) by using different combination of input features data set – per unit RMS values, fundamental and third harmonic components of 3 phase current and voltage – in MATLAB programming environment.

Furthermore, total of 8 experiments are conducted. In each experiment, per unit RMS value, fundamental and third harmonic components of 3 phase current and voltage values are calculated every 0.1s. Therefore, there are total of 690 data samples. Among them, 70% of input features data are used for training, 30% of input features data are used for validation and testing. Percentage error of training, validation and testing states for all 8 experiments are shown

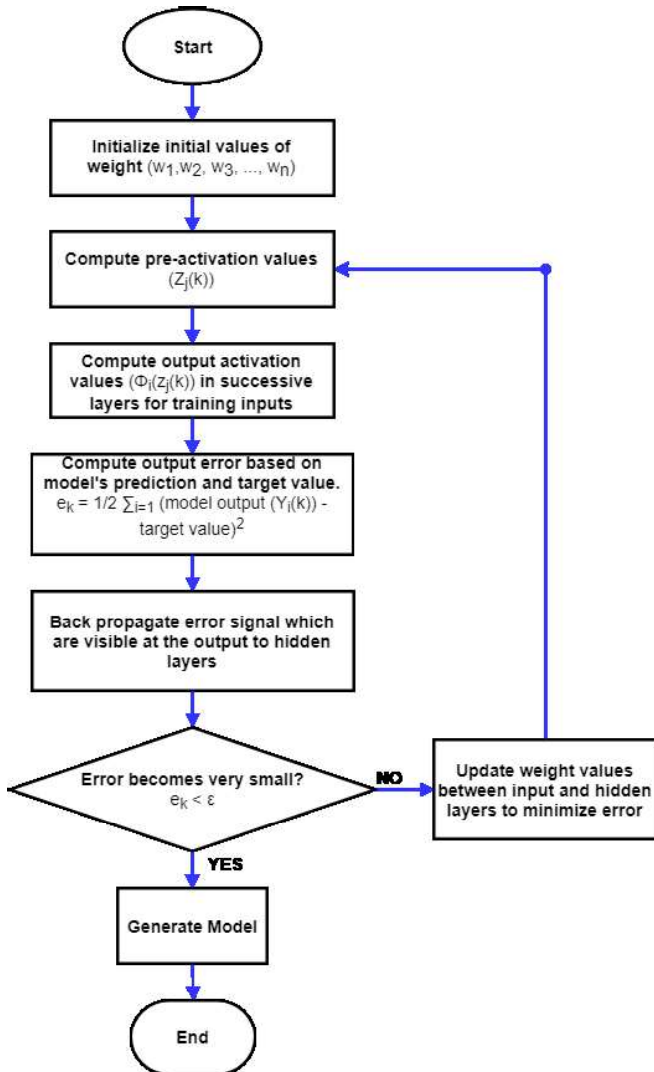


Fig. 8. Flowchart of feedforward neural network

in table 4. However, only 2 experiment results out of 8 will be explained in detail in this section.

A. Experiment 1

In this experiment, 2 layers neural network is trained by using per unit RMS values of 3 phase current and voltage, $[I_{a_{rms}}, I_{b_{rms}}, I_{c_{rms}}, V_{a_{rms}}, V_{b_{rms}}, V_{c_{rms}}]$. The numbers of hidden neurons which are used to train, validate and test in this experiment are 12. Fig. 10 shows structured of the used 2 layers neural network. In addition, fig. 11 shows how errors in training, validation and testing states reduce as the number of iteration increases. It can be seen from fig. 11 that it takes 94 loop iterations to achieve best validation performance.

In addition, fig. 12 shows confusion matrix of classification model during training, testing and validation. The confusion matrices show performance of classification model. In confusion matrix, rows represent predictions of different classes from classification model and columns represent actual classes. The green squares are properly classified percentage for each class, but red squares indicate misclassified percentage. The blue square shows total percentage of correct and incorrect classification. For example, in fig. 12, during training, classification model misclassifies 0.4% of class 2 data as class 1, misclassifies 0.2% of class3 data as class 2, and misclassifies 0.4% of class 4 data as class 3 and so on. Hence, in overall, classification model can correctly classify 98.3% during training. Next, classification model can correctly classify 100% during validation state and finally, in testing state, classification model misclassifies 1% of class 6 data as class 5 in testing state.

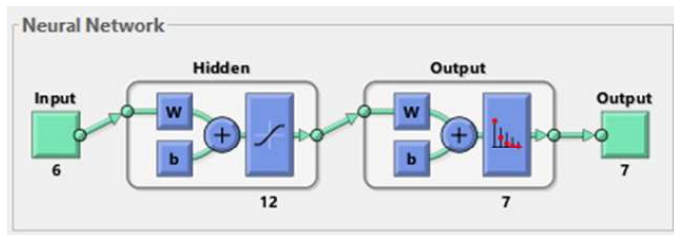


Fig. 10. Structure of 2 layers neural network

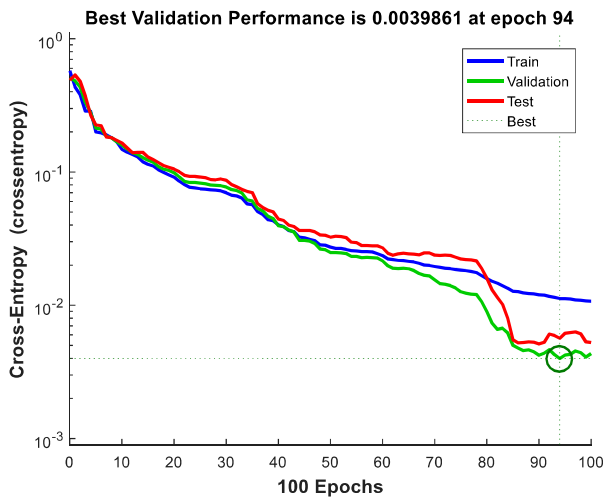


Fig. 11. Performance graph

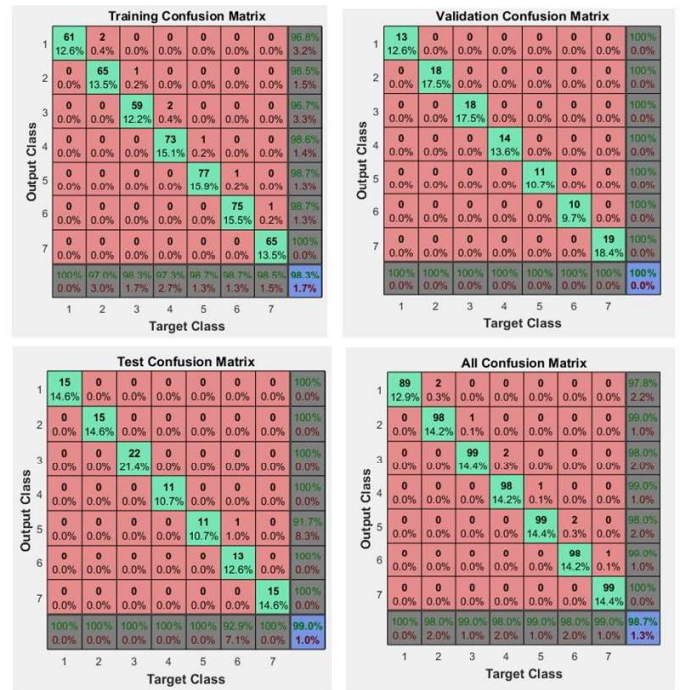


Fig. 12. Confusion matrices

Moreover, fig. 13 shows receiver operating characteristics plot, ROC. ROC plot shows percentage of true positive class prediction that classification model can classify as a function of acceptable number of false positive classification. Closer the line to the left side and top side, the better is classification model.

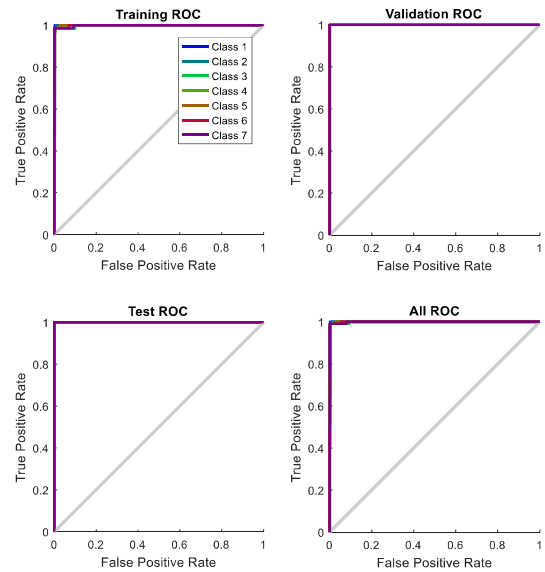


Fig. 13. Receiver operation characteristics, ROC

Table 2 shows cross-entropy and percentage error results of classification model. Cross-entropy measures performance of a classification model which is the distance between probability vector of classes from classification model output and target vector. The smaller the cross-entropy values are, the better classification result is. Percentage error also indicates the fraction of samples which are misclassified.

Table 2. Cross-Entropy and percentage error

Results	Cross-Entropy	Percentage error
Training	4.40056	1.65631
Validation	12.59484	0
Testing	12.60490	0.970873

B. Experiment 2

In this experiment, the 2 layers neural network is trained by using per unit RMS value, fundamental and third harmonic components of 3 phases current and voltage – [$I_{a_{rms}}, I_{b_{rms}}, I_{c_{rms}}, V_{a_{rms}}, V_{b_{rms}}, V_{c_{rms}}, I_{a_{fl}}, I_{b_{fl}}, I_{c_{fl}}, I_{a_{\beta 3}}, I_{b_{\beta 3}}, I_{c_{\beta 3}}, V_{a_{fl}}, V_{b_{fl}}, V_{c_{fl}}, V_{a_{\beta 3}}, V_{b_{\beta 3}}, V_{c_{\beta 3}}$] taken from healthy and turn-to-turn stator winding short circuit fault condition and the number of hidden neuron used in this experiment are 18.

Fig. 14 shows confusion matrices of classification model during training, testing and validation. During training state, the classification model misclassifies 0.4% of class 2 data as class 1 data, misclassifies 0.2% of class 4 data as class 3, misclassifies 0.2% of class 5 data as class 4 data and misclassifies 0.2% of class 7 data as class 6 data. Furthermore, during validation state, only 1% of class 3 data is misclassified as class 2 data and finally, 1.9% of class 3 data is misclassified as class 2 data and 1% of class 7 data as class 6 data by classification model in testing state.

Moreover, fig. 15 shows receiver operating characteristics plot, ROC. Closer the line to the left side and top side, the better is classification model. Next, table 3 shows cross-entropy and percentage error results of the classification model. As compare with previous experiment, when the number of input features increases, cross-entropy value and percentage error during validation and testing states increases.

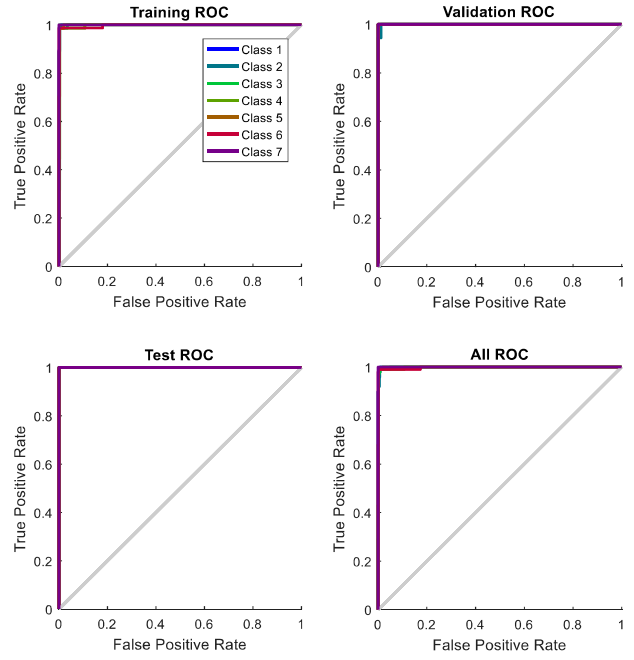


Fig. 15. Receiver operating characteristics, ROC

Table 3. Cross-Entropy and percentage error

Results	Cross-Entropy	Percentage error
Training	4.36502	1.65631
Validation	12.89522	0.970873
Testing	12.85344	2.91262

C. Experiment Results

This section will show all experiment results of cross-entropy and percentage error on training, validation, and testing of neural network due to change in number of input features and number of hidden neurons.

Table 4. Summary of neural network model performances based on number of different input features and hidden neurons

Experiment s	No: of hidden neurons	Input features	Cross-Entropy	Percentage error
Experiment 1	12	$I_{a_{rms}}, I_{b_{rms}}, I_{c_{rms}}, V_{a_{rms}}, V_{b_{rms}}, V_{c_{rms}}$	Training = 4.4006	Trainin g = 1.6563
			Validation = 12.5948	Validat ion = 0
			Testing = 12.6049	Testing = 0.97987
Experiment 2	18	$I_{a_{rms}}, I_{b_{rms}}, I_{c_{rms}}, V_{a_{rms}}, V_{b_{rms}}, V_{c_{rms}}$	Training = 4.365	Trainin g = 1.6563
			Validation = 12.8952	Validat ion =

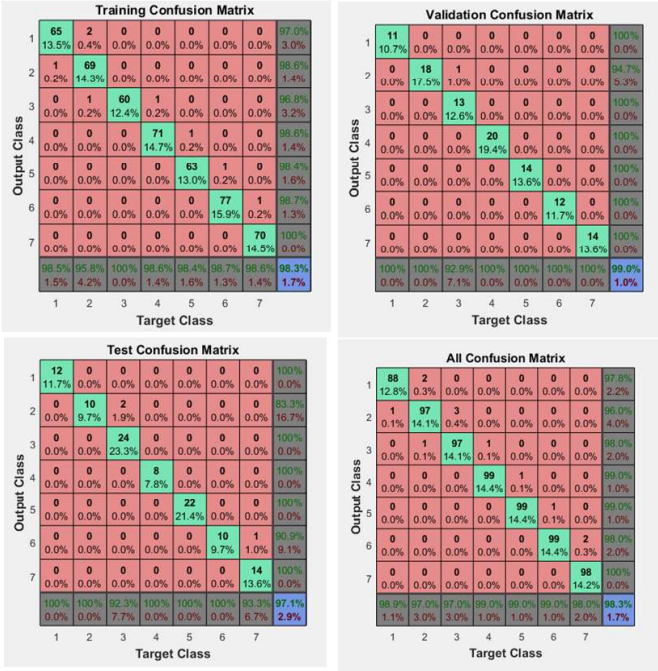


Fig. 14. Confusion matrices

		Ia _{f1} , Ia _{f3} , Ib _{f1} , Ib _{f3} , Ic _{f1} , Ic _{f3} , Va _{f1} , Va _{f3} , Vb _{f1} , Vb _{f3} , Vc _{f1} , Vc _{f3} .	Testing = 12.8534	0.9798 7 Testing = 2.9126
Experiment 3		Ia _{rms} , Ib _{rms} , Ic _{rms} , Ia _{f1} , Ia _{f3} , Ib _{f1} , Ib _{f3} , Ic _{f1} , Ic _{f3}	Training = 4.5745 Validatio n = 13.1825 Testing = 13.3742	Trainin g = 2.2774 Validat ion = 2.9126 Testing = 3.8835
Experiment 4		Va _{rms} , Vb _{rms} , Vc _{rms} , Va _{f1} , Va _{f3} , Vb _{f1} , Vb _{f3} , Vc _{f1} , Vc _{f3}	Training = 3.0784 Validatio n = 8.8114 Testing = 8.72689	Trainin g = 2.8986 Validat ion = 4.8544 Testing = 2.9126
Experiment 5		Ia _{rms} , Ib _{rms} , Ic _{rms} , Va _{rms} , Vb _{rms} , Vc _{rms}	Training = 4.2429 Validatio n = 12.0973 Testing = 11.9668	Trainin g = 1.4493 Validat ion = 0.9708 7 Testing = 3.8835
Experiment 6	36	Ia _{rms} , Ib _{rms} , Ic _{rms} , Va _{rms} , Vb _{rms} , Vc _{rms} , Ia _{f1} , Ia _{f3} , Ib _{f1} , Ib _{f3} , Ic _{f1} , Ic _{f3} , Va _{f1} , Va _{f3} , Vb _{f1} , Vb _{f3} , Vc _{f1} , Vc _{f3} .	Training = 4.6409 Validatio n = 13.3229 Testing = 13.2371	Trainin g = 1.8634 Validat ion = 2.9126 Testing = 0.9708 7
Experiment 7		Ia _{rms} , Ib _{rms} , Ic _{rms} , Ia _{f1} , Ia _{f3} , Ib _{f1} , Ib _{f3} , Ic _{f1} , Ic _{f3}	Training = 4.9942 Validatio n = 14.3898 Testing =	Trainin g = 1.6563 Validat ion = 0.9708

			14.5232	7 Testing = 1.9417
Experiment 8		Va _{rms} , Vb _{rms} , Vc _{rms} , Va _{f1} , Va _{f3} , Vb _{f1} , Vb _{f3} , Vc _{f1} , Vc _{f3}	Training = 4.7225 Validatio n = 13.4469 Testing = 13.4508	Trainin g = 1.8634 Validat ion = 0.9708 7 Testing = 3.8835

From table 4, it can be seen that when number of hidden neuron increases, cross-entropy value in experiments using per unit RMS values of 3 phase current and voltage in experiment 1 and 5 decreases whereas cross-entropy values in other experiments increases. It can also be seen that per unit RMS values of 3 phases current and voltage seems to be better input features than harmonic components for this application because the amount of samples which are misclassified in experiment 1 is smaller than other experiments.

VII. CONCLUSION

In this project, different features such as per unit RMS value, fundamental and third harmonic components of 3 phases stator current and 3 phases voltage from healthy and faulty condition of synchronous generator are extracted, trained, tested and validated the classification neural network model. The experiment results show that feedforward neural network can be used efficiently to classify between healthy and different stator winding fault levels. Last, but not least, this project explores only turn-to-turn stator winding short circuit fault in 3 phase synchronous generator with linear load by using electrical signals (current and voltage) and 2 layers neural network. Effects on non-linear load on healthy and turn-to-turn stator winding fault machine conditions could explored further by using multilayer neural network and more input signals such as current, voltage, vibration, machine angular speed and so on.

ACKNOWLEDGMENT

The team would like to take this opportunity to thank Rolls-Royce Electrical, Singapore and Nanyang Technological University, Singapore for supporting the team with world class lab facility to facilitate in researching cutting edge technologies.

REFERENCES

- [1] F. Immovilli, A. Bellini, R. Rubini and C. Tassoni, "Diagnosis of Bearing Faults in Induction Machines by Vibration or Current Signals: A Critical Comparison," in *IEEE Transactions on Industry Applications*, vol. 46, no. 4, pp. 1350-1359, July-Aug. 2010.
- [2] Y. Gritli, A. O. Di Tommaso, R. Miceli, F. Filippetti and C. Rossi, "Closed-loop bandwidth impact on MVSA for rotor broken bar diagnosis in IRFOC double squirrel cage induction motor drives," *2013 International Conference on Clean Electrical Power (ICCEP)*, Alghero, 2013, pp. 529-534.

- [3] P. Nivesrangsan and D. Jantarajirojkul, "Bearing fault monitoring by comparison with main bearing frequency components using vibration signal," *2018 5th International Conference on Business and Industrial Research (ICBIR)*, Bangkok, 2018, pp. 292-296.
- [4] N. Sivakumar, S. K. Panda, B. Bicky and Amit Kumar Gupta, "Hybrid Model for Wound-Rotor Synchronous Generator to Detect and Diagnose Turn-to-Turn Short-Circuit Fault in Stator Windings," *IEEE*, vol. 62, no. 3, pp. 1888 - 1900, 2014.
- [5] IEEE Recommended Practice for the Design of Reliable Industrial and Commercial Power Systems," in *IEEE Std 493-2007 (Revision of IEEE Std 493-1997) - Redline*, vol., no., pp.1-426, 25 June 2007
- [6] I. F. El-Arabawy, M. I. Masoud and A. E. Mokhtari, "Stator Inter-turn Faults Detection and Localization Using Stator Currents and Concordia Patterns - Neural Network Applications," *2007 Compatibility in Power Electronics*, Gdansk, 2007, pp. 1-7.
- [7] S. Morsalin, K. Mahmud, H. Mohiuddin, M. R. Halim and P. Saha, "Induction motor inter-turn fault detection using heuristic noninvasive approach by artificial neural network with Levenberg Marquardt algorithm," *2014 International Conference on Informatics, Electronics & Vision (ICIEV)*, Dhaka, 2014, pp. 1-6.
- [8] M. Kande, A. J. Isaksson, R. Thottappillil and N. Taylorn, "Rotating Electrical Machine Condition Monitoring Automation - A Review," *Machine*, 2017.
- [9] S. Nadarajan, R. Wang, A. Kumar Gupta and S. Kumar Panda, "Vibration signature analysis of stator winding fault diagnosis in brushless synchronous generators," *2015 IEEE International Transportation Electrification Conference (ITEC)*, Chennai, 2015, pp. 1-6.
- [10] J. Sottile, F. C. Trutt and A. W. Leedy, "Condition Monitoring of Brushless Three-Phase Synchronous Generators With Stator Winding or Rotor Circuit Deterioration," in *IEEE Transactions on Industry Applications*, vol. 42, no. 5, pp. 1209-1215, Sept.-Oct. 2006.
- [11] P. J. Broniera, W. S. Gongora, A. Goedel and W. F. Godoy, "Diagnosis of stator winding inter-turn short circuit in three-phase induction motors by using artificial neural networks," *2013 9th IEEE International Symposium on Diagnostics for Electric Machines, Power Electronics and Drives (SDEMPED)*, Valencia, 2013, pp. 281-287.
- [12] "Patternnet," The MathWorks, Inc., [Online]. Available: <https://www.mathworks.com/help/nnet/ref/patternnet.html>. [Accessed 01 April 2018].
- [13] A. Gandhi, T. Corrigan and L. Parsa, "Recent Advances in Modeling and Online Detection of Stator Interturn Faults in Electrical Motors," in *IEEE Transactions on Industrial Electronics*, vol. 58, no. 5, pp. 1564-1575, May 2011.
- [14] B. Aubert, J. Regnier, S. Caux and D. Alejo, "On-line inter-turn short-circuit detection in permanent magnet synchronous generators," *2013 9th IEEE International Symposium on Diagnostics for Electric Machines, Power Electronics and Drives (SDEMPED)*, Valencia, 2013, pp. 329-335.
- [15] B. Aubert, J. Régnier, S. Caux and D. Alejo, "Kalman-Filter-Based Indicator for Online Interturn Short Circuits Detection in Permanent-Magnet Synchronous Generators," in *IEEE Transactions on Industrial Electronics*, vol. 62, no. 3, pp. 1921-1930, March 2015.